The Astrophysical Journal, 637:242–254, 2006 January 20

UV DUST ATTENUATION IN NORMAL STAR-FORMING GALAXIES. I. ESTIMATING THE L_{TIR}/L_{FUV} RATIO

L. Cortese,[1,2] A. Boselli,[1] V. Buat,[1] G. Gavazzi,[2] S. Boissier,[3] A. Gil de Paz,[3] M. Seibert,[4] B. F. Madore,[3,5] and D. C. Martin[4]

Received 2005 June 15; accepted 2005 September 20

ABSTRACT

We analyze the dust attenuation properties of a volume-limited, optically selected sample of normal star-forming galaxies in nearby clusters as observed by *GALEX*. The internal attenuation is estimated using three independent indicators, namely, the ratio of the total infrared to far-ultraviolet emission, the ultraviolet spectral slope β, and the Balmer decrement. We confirm that normal galaxies follow a L_{TIR}/L_{FUV}-β relation offset from the one observed for starburst galaxies. This offset is found to weakly correlate with the birthrate parameter and thus with the galaxy star formation history. We study the correlations of dust attenuation with other global properties, such as the metallicity, dynamical mass, ionized gas attenuation, Hα emission, and mass surface density. Metal-rich, massive galaxies are, as expected, more heavily extinguished in the UV than are small systems. For the same gas metallicity normal galaxies have lower L_{TIR}/L_{FUV} ratios than starbursts, in agreement with the difference observed in the L_{TIR}/L_{FUV}-β relation. Unexpectedly, however, we find that normal star-forming galaxies follow exactly the same relationship between metallicity and ultraviolet spectral slope β determined for starbursts, complicating our understanding of dust properties. This result might indicate a different dust geometry between normal galaxies and starbursts, but it could also be due to aperture effects eventually present in the *IUE* starbursts data set. The present multiwavelength study allows us to provide some empirical relations from which the total infrared to far-ultraviolet ratio (L_{TIR}/L_{FUV}) can be estimated when far-infrared data are absent.

Subject headings: dust, extinction — galaxies: spiral — galaxies: starburst — ultraviolet: galaxies

Online material: color figures

1. INTRODUCTION

The presence of dust in galaxies represents one of the major obstacles complicating a direct quantification of the star formation activity in local and high-redshift galaxies. Absorption by dust grains reddens the spectra at short wavelengths and modifies altogether the spectral energy distribution of galaxies. Since the UV radiation is emitted by young stars ($t < 10^8$ yr) that are generally more affected by attenuation from surrounding dust clouds than older stellar populations, rest-frame UV observations can lead to incomplete and/or biased reconstructions of the star formation activity and star formation history of galaxies affected by dust absorption, unless proper corrections are applied. In recent years our understanding of dust attenuation received a tremendous impulse from studies of local starburst galaxies (i.e., Calzetti et al. 1994; Heckman et al. 1998; Meurer et al. 1999; Calzetti 2001; Charlot & Fall 2000) that were based on three indicators: the ratio of the total infrared to far-ultraviolet emission (L_{TIR}/L_{FUV}), the ultraviolet spectral slope β (determined from a power-law fit of the form $f \sim \lambda^{\beta}$ to the UV continuum spectrum in the range 1300 and 2600 Å (Calzetti et al. 1994), and the Balmer decrement. The total IR (TIR) to UV luminosity ratio method (i.e., Buat 1992; Xu & Buat 1995; Meurer et al. 1995, 1999) is based on the assumption that a fraction of photons emitted by stars and gas are absorbed by the dust. The dust heats up and subsequently reemits the energy in the mid- and far-infrared. The amount of UV attenuation can thus be quantified by means of an energy balance. This method is considered the most reliable estimator of the dust attenuation in star-forming galaxies because it is almost completely independent of the assumed extinction mechanisms (i.e., dust/star geometry, extinction law; see Buat & Xu 1996; Meurer et al. 1999; Gordon et al. 2000; Witt & Gordon 2000). When the spectrum is dominated by a young stellar population, the ultraviolet spectral slope β, is found to have a weak dependence on metallicity, initial mass function, and star formation history (Leitherer & Heckman 1995). Thus the difference between the observed β and the one predicted by models can be entirely ascribed to dust attenuation (Meurer et al. 1999). However, in systems with no or mild star formation activity the UV spectral slope can be strongly contaminated by the old stellar populations, whose contribution increases β (i.e., flattens the UV continuum; Boissier et al. 2005). Thus the spectral slope of mildly star-forming systems could be intrinsically different from the one of starburst galaxies, even in the absence of dust attenuation (Kong et al. 2004). Meurer et al. (1999) have shown that in starburst galaxies the total far-infrared (FIR) to ultraviolet luminosity ratio correlates with the ultraviolet spectral slope, β (commonly referred to as the infrared excess–UV [IRX-UV] relation). They pointed out that this relation allows reliable estimates of the attenuation by dust at ultraviolet wavelengths based on β. The Balmer decrement gives an estimate of the attenuation of ionized gas, and not of the stellar continuum as in the previous two methods. It is based on the comparison of the observed Hα/Hβ ratio with its predicted value (2.86 for case B recombination, assuming an electronic density $n_e \leq 10^4$ cm^{-3} and temperature $\sim 10^4$ K; e.g., Osterbrock 1989). Calzetti et al. (1994) found a

[1] Laboratoire d'Astrophysique de Marseille, BP8, Traverse du Siphon, F-13376 Marseille, France.

[2] Università degli Studi di Milano-Bicocca, Piazza della Scienza 3, 20126 Milano, Italy.

[3] Observatories of the Carnegie Institution of Washington, 813 Santa Barbara Street, Pasadena, CA 91101.

[4] California Institute of Technology, MC 405-47, 1200 East California Boulevard, Pasadena, CA 91125.

[5] NASA/IPAC Extragalactic Database, California Institute of Technology, Mail Code 100-22, 770 South Wilson Avenue, Pasadena, CA 91125.

significant correlation between the ultraviolet spectral slope β and the Balmer decrement Hα/Hβ. Starting from this empirical relation they obtained an attenuation law (known as the Calzetti attenuation law) often adopted to correct UV observations for dust attenuation in absence of both FIR observations and estimates of the ultraviolet spectral slope (Steidel et al. 1999; Glazebrook et al. 1999). Unfortunately, the above empirical relations have been established only for starburst galaxies, and they seem not to hold for normal star-forming galaxies. Recently, Bell (2002) suggested that quiescent galaxies deviate from the IRX-UV relation of starburst galaxies, because they tend to have redder ultraviolet spectra at fixed total FIR to ultraviolet luminosity ratio. Kong et al. (2004) confirmed this result and interpreted the different behavior of starbursts and normal galaxies as due to a difference in the star formation histories. They proposed that the offset from the starburst IRX-UV relation can be predicted using the birthrate parameter b (e.g., the ratio of the current to the mean past star formation activity). However, an independent observational confirmation of the correlation between the distance from the starburst IRX-UV relation and the birthrate parameter has not been obtained so far (Seibert et al. 2005). Even the Calzetti law does not seem to be universal. Buat et al. (2002) showed that for normal star-forming galaxies the attenuation derived from the Calzetti law is $\sim$0.6 mag larger than the one computed from the $F_{\rm FIR}/F_{\rm UV}$ ratio and their result has been recently confirmed by Laird et al. (2005). Why do normal star-forming galaxies behave differently from starbursts? Do normal galaxies follow different empirical relations that can be exploited to correct for dust attenuation in absence of FIR observations? If this is the case, is there a transition between starburst and normal galaxies? Which physical parameters drive it? Answering these questions will be important for a better understanding of the interaction of dust and radiation specifically in nearby dusty star-forming galaxies, but it also has direct consequences for our understanding and interpretation of galaxy evolution in a general context. First, it seems mandatory to characterize the dust attenuation properties of normal galaxies, to compare them with the ones of starbursts and to derive new recipes for the UV dust attenuation correction. This topic came once again to the fore with the launch of the *Galaxy Evolution Explorer* (*GALEX*). This satellite is delivering to the community an unprecedented amount of UV data on local and high-redshift galaxies that require corrections for dust attenuation but currently lack FIR rest-frame data. The time is ripe to explore new methods for correction of these data, that might provide new insights on galaxy evolution. Whenever they can be combined with other data, *GALEX* observations provide the best available ultraviolet data for studying the dust attenuation properties of galaxies. Multiwavelength photometric and spectroscopic observations are in fact mandatory in order to determine metallicity, ionized gas attenuation [A(Hα)], luminosity, and mass; to test the validity of the relations followed by starbursts (Heckman et al. 1998); and to explore relations that might prove useful to correct ultraviolet magnitudes and compare them with various models of dust attenuation. Recent extensive spectroscopic and photometric surveys, such as the Sloan Digital Sky Survey (SDSS; Abazajian et al. 2005) and the Two Degree Field Galaxy Redshift Survey (2dF; Colless et al. 2001), have opened the path to studies of fundamental physical parameters based on enormous data sets. However, spectroscopic observations of nearby galaxies suffer from strong aperture effects, making these data sets not ideal for the purpose of the present investigation. In fact, Kewley et al. (2005) have recently shown that aperture effects produce both systematic and random errors on the estimate of star formation, metallicity, and attenuation. To reduce at least the systematic effects they suggest selecting only samples with fibers that capture >20% of the light. This requires $z > 0.04$ and $z > 0.06$ for SDSS and 2dF, respectively—too distant to detect both giant and dwarf star-forming systems with *GALEX* and *IRAS* (*Infrared Astronomical Satellite*). Although significantly smaller than the SDSS, the data set that we have been building up over the last 10 years with data taken over a large stretch of the electromagnetic spectrum for few thousand galaxies in the local universe (worldwide available from the site GOLDMine; Gavazzi et al. 2003) turns out to be appropriate for the purposes of the present investigation. It includes drift-scan mode integrated spectra, narrowband Hα and broadband optical and near-infrared (NIR) imaging for a volume-limited sample of nearby galaxies in and outside rich clusters. The combination of *GALEX* and *IRAS* observations with these ancillary data allows us to study the dust attenuation properties in a sizable sample of normal star-forming galaxies not suffering from the aperture bias and to compare observations with model predictions.

In this first paper we investigate the relations between dust attenuation and global galaxy properties and compare them with the ones observed in starburst galaxies. The aim of this work is to provide some empirical relations based on observable (and thus model-independent) quantities suitable for deriving dust attenuation corrections when FIR data are not available. For this reason all relations obtained throughout this paper are given as a function of $L_{\rm TIR}/L_{\rm FUV}$, the observable that we consider the best dust attenuation indicator. We choose not to transform $L_{\rm TIR}/L_{\rm FUV}$ into a (model-dependent) estimate of the far-ultraviolet extinction A(FUV), leaving the reader free to choose his/her preferred dust model (i.e., Meurer et al. 1999; Buat et al. 1999, 2002, 2005; Gordon et al. 2000; Panuzzo et al. 2003; Burgarella et al. 2005; A. K. Inoue et al. 2006, in preparation). Throughout the paper we assume that quantities are related linearly and residual plots are presented in order to test the validity of this hypothesis. Moreover, since we are looking for new recipes to estimate the $L_{\rm TIR}/L_{\rm FUV}$ ratio, this quantity has to be considered as the dependent variable, implying the use of an unweighted simple linear fit to estimate the best-fitting parameters (Isobe et al. 1990). A forthcoming paper will be focused on the comparison between models and observations hoping to gain a better understanding on the physics of dust attenuation and to study new recipes useful to convert $L_{\rm TIR}/L_{\rm FUV}$ into A(FUV).

2. THE DATA

2.1. *The Optically Selected Sample*

The analysis presented in this work is based on an optically selected sample of late-type galaxies (later than S0a) including giant and dwarf systems extracted from the Virgo Cluster Catalog (VCC; Binggeli et al. 1985) and from the CGCG (Catalog of Galaxies and Clusters of Galaxies; Zwicky et al. 1961). The data include $\sim$300 deg^2 covering most of the Virgo, Abell 1367, and Abell 262 Clusters, the southwest part of the Coma Cluster, and part of the Coma–Abell 1367 supercluster ($11^{\rm h}30^{\rm m} <$ R.A. $< 13^{\rm h}30^{\rm m}$, $18^\circ <$ decl. $< 32^\circ$) observed in spring 2004 as part of the All-Sky Imaging Survey (AIS) and of the Nearby Galaxy Survey (NGS) carried out by *GALEX* in two UV bands: far-ultraviolet (FUV; $\lambda_{\rm eff} = 1530$ Å, $\Delta\lambda = 400$ Å) and near-ultraviolet (NUV; $\lambda_{\rm eff} = 2310$ Å, $\Delta\lambda = 1000$ Å). Details of the *GALEX* instrument and characteristics can be found in Martin et al. (2005) and Morrissey et al. (2005). Our sample has the quality of being selected with the criterion of optical completeness. All galaxies brighter than a threshold magnitude are selected in all areas. In the Coma–Abell 1367 supercluster and A262 Cluster all galaxies brighter than $m_p = 15.7$ were selected

from the CGCG (Zwicky et al. 1961). The Virgo region contains all galaxies brighter than $m_p = 18$ from the VCC (Binggeli et al. 1985). We thus consider our sample an optically selected, volume-limited sample. We include in our analysis all late-type galaxies, detected in both NUV and FUV *GALEX* bands and in both 60 and 100 μm *IRAS* bands (157 objects). Whenever available, we extracted UV fluxes from the deep NGS images, obtained with a mean integration time of $\sim$1500 s, complete to $m_{\rm AB} \sim 21.5$ in the NUV and FUV. Elsewhere UV fluxes have been extracted from the shallower AIS images ($\sim$70 deg^2), obtained with a mean integration time of $\sim$100 s, complete to $m_{\rm AB} \sim 20$ in both the FUV and NUV bands. All UV images come from the Internal Data Release version 1 (IR1.0). UV fluxes were obtained by integrating *GALEX* images within elliptical annuli of increasing diameter up to the optical *B* band 25 mag arcsec^{-2} isophotal radii, consistently with the optical and NIR images. Independent measurements of the same galaxies obtained in different exposures give consistent photometric results within 10% in the NUV and 15% in the FUV in the AIS, and a factor of $\sim$2 better for bright (NUV $\leq$ 16) galaxies. The uncertainty in the UV photometry is on average a factor of $\sim$2 better in the NGS than in the AIS, particularly for faint objects. The typical uncertainty in the *IRAS* data is 15% (Boselli et al. 2003). UV and FIR data have been combined to multifrequency data. These are optical and NIR H imaging (mostly from Gavazzi et al. 2000, 2005; Boselli et al. 2003), optical drift-scan spectra (Gavazzi et al. 2004), and Hα imaging (Boselli & Gavazzi 2002; Boselli et al. 2002a; Gavazzi et al. 1998, 2002b, 2006; Iglesias-Páramo et al. 2002), a great part of which are available from the GOLDMine galaxy database (Gavazzi et al. 2003).[6] From the 157 galaxies selected we exclude active galactic nuclei (AGNs). AGNs have been selected using either the classification provided by NED, if available, or by inspection to the integrated spectra of Gavazzi et al. (2004): we exclude galaxies with $\log([{\rm O\ III}]/{\rm H}\beta) > 0.61/[\log([{\rm N\ II}]/{\rm H}\alpha) - 0.05] + 1.3$ (Kauffmann et al. 2003). This criterion reduces the sample to 128 galaxies, spanning a range of 6 mag in *B* band ($-22 < M_B < -16$) and 3 orders of magnitude in mass ($9 < M < 12\ {\rm M}_\odot$).[7] Unfortunately, ancillary data are not available for all galaxies observed by *GALEX*; we thus further divided the data in two subsamples. Sixty-six galaxies in the "primary sample" have all the necessary complementary data (e.g., Hα photometry, Hα/Hβ ratio, metallicity, and *H*-band photometry; see Gavazzi et al. 2000, 2002a, 2002b, and 2004 for the selection criteria adopted in each survey). The remaining 62 galaxies form the "secondary sample."

We cannot exclude a possible contamination of AGNs in the secondary sample, since no spectra are available for these objects. In all figures objects belonging to the primary sample are indicated with filled circles, while the secondary sample is indicated as empty circles. Since only galaxies belonging to the primary sample are present in all the plots analyzed in the presented work, all correlations are quantified using only the primary sample. Data from UV to NIR have been corrected for Galactic extinction according to Burstein & Heiles (1982). We assume a distance of 17 Mpc for the members of Virgo Cluster A, 22 Mpc for Virgo Cluster B, and 32 Mpc for objects in the M and W clouds (Gavazzi et al. 1999). Members of the Cancer, Abell 1367, and Coma Clusters are assumed to lie at distances of 65.2, 91.3, and 96 Mpc, respectively. Isolated galaxies in the Coma–Abell 1367 supercluster are assumed at their redshift distance, adopting $H_0 = 75$ km s^{-1} Mpc^{-1}.

[6] See http://goldmine.mib.infn.it.

[7] Computed using the relation between L_H and M by Gavazzi et al. (1996).

2.2. *The Starburst Sample*

In order to compare the properties of our sample with starbursts, we compile a data set of starburst galaxies observed by *IUE* (*International Ultraviolet Explorer*) from the sample of Calzetti et al. (1994). We consider 29 galaxies, excluding AGNs and galaxies that have not been observed by *IRAS* at 60 or 100 μm. Complementary data such as FIR, Hα fluxes and Balmer decrements are taken from Calzetti et al. (1995), metallicities come from Heckman et al. (1998), and *H*-band photometry (available only for 18 galaxies) come from Calzetti (1997). Excluding the FIR fluxes, all these quantities are obtained within an apertures of $\sim 20 \times 10$ arcsec^2, consistent with *IUE* observations (Calzetti et al. 1994). Thus we stress that aperture effects could strongly affect any comparison with normal galaxies for which all data are homogeneously integrated values. First of all, if the UV emission is more extended than *IUE* field of view the $L_{\rm TIR}/L_{\rm FUV}$ ratio is overestimated.[8] In addition, even when physical quantities are obtained in the same *IUE* apertures, the presence of age and metallicity gradients in galaxies makes not trivial any comparison with the integrated values obtained for normal star-forming galaxies (Kewley et al. 2005). All the observables except the ultraviolet spectra slope β are calibrated in a way consistent with our sample of normal galaxy. The ultraviolet spectral slope of starbursts is obtained by fitting *IUE* spectra (Calzetti et al. 1994), while for *GALEX* observations it comes from the FUV-NUV color index (see next section). However, as shown by Kong et al. (2004), these two calibrations are consistent each other and do not introduce any systematic difference between the two samples.

3. THE $L_{\rm TIR}/L_{\rm FUV}$-β RELATION FOR NORMAL STAR-FORMING GALAXIES

Meurer et al. (1999) have shown that the ratio of FIR to FUV luminosity tightly correlates with the UV colors of starburst galaxies. This relation, known as IRX-UV relation, is often presented as β versus the $L_{\rm TIR}/L_{\rm FUV}$ relation. As discussed in the introduction, we refer throughout this paper to the $L_{\rm TIR}/L_{\rm FUV}$ ratio as the best indicator of UV dust attenuation, and we calibrate on it all the following relations. In order to determine the dust emission, we compute the total infrared flux emitted in the range 1–1000 μm, following Dale et al. (2001):

$$\log(f_{\rm TIR}) = \log(f_{\rm FIR}) + 0.2738 - 0.0282 \log\left(\frac{f_{60}}{f_{100}}\right) + 0.7281 \log\left(\frac{f_{60}}{f_{100}}\right)^2 + 0.6208 \log\left(\frac{f_{60}}{f_{100}}\right)^3 + 0.9118 \log\left(\frac{f_{60}}{f_{100}}\right)^4, \quad (1)$$

where $f_{\rm FIR}$ is the FIR flux, defined as the flux between 42 and 122 μm (Helou et al. 1988),

$$f_{\rm FIR} = 1.26(2.58 f_{60} + f_{100}) \times 10^{-14}\ \left({\rm W\ m^{-2}}\right), \quad (2)$$

and f_{60} and f_{100} are the *IRAS* fluxes measured at 60 and 100 μm (in Jansky). The total infrared luminosity is thus

$$L_{\rm TIR} = 4\pi D^2 f_{\rm TIR}. \quad (3)$$

The β-parameter as determined from *GALEX* colors is very sensitive to the galaxy star formation history (see, for example,

[8] However, Meurer et al. (1999) argued that the majority of UV flux for their starburst sample lies within the *IUE* aperture.

Calzetti et al. 2005). For this reason we assume throughout this paper β as defined by Kong et al. (2004):

$$\beta = \frac{\log(f_{\rm FUV}) - \log(f_{\rm NUV})}{-0.182} = 2.201({\rm FUV} - {\rm NUV}) - 1.804, \quad (4)$$

where $f_{\rm FUV}$ and $f_{\rm NUV}$ are the NUV and FUV observed fluxes, respectively (in ergs cm^2 s^{-1} Å^{-1}), and FUV and NUV are the observed magnitudes. The relationship between the ratio of total infrared luminosity ($L_{\rm TIR}$) obtained from equation (1) to the FUV fluxes and the UV spectral slope β (or the FUV-NUV color) for our sample of nearby star-forming galaxies is given in Figure 1. Several functional forms of the $L_{\rm TIR}/L_{\rm FUV}$-β relation can be found in the literature (i.e., Meurer et al. 1999; Kong et al. 2004); we simply adopt a linear fit: $\log(L_{\rm TIR}/L_{\rm FUV}) = a\beta + b$. This functional form is consistent with other previously proposed for $\beta > -2$, while it diverges for $\beta < -2$. Since the majority of normal and starbursts galaxies have $\beta > -2$, our choice is justified. This represents the simplest and least parameter-dependent way to study the relation between two quantities.[9] We find a strong correlation [Spearman correlation coefficient $r_s \sim 0.76$ for the primary sample and $r_s \sim 0.65$ for the secondary sample, both corresponding to a probability $P(r_s) > 99.9\%$ that the two variables are correlated] between the total infrared to FUV ratio and the spectral slope, but significantly different from the one observed for starburst galaxies (Fig. 1, *dashed line*; Meurer et al. 1999). A χ^2 test rejects at a confidence level higher than 99.9% that the two samples follow the same relation. The best linear fit for our primary sample (Fig. 1, *solid line*) is

$$\log\left(\frac{L_{\rm TIR}}{L_{\rm FUV}}\right) = (0.70 \pm 0.06)\beta + (1.30 \pm 0.06). \quad (5)$$

The uncertainty in the estimate of the $L_{\rm TIR}/L_{\rm FUV}$ using equation (5) is $\sim$0.26 $\pm$ 0.02 dex for the primary sample, but it increases to $\sim$0.35 $\pm$ 0.03 dex if we consider the whole sample (e.g., primary and secondary samples), consistent with the mean uncertainty observed for starburst galaxies (Meurer et al. 1999). A large contribution ($\sim$0.21 $\pm$ 0.02 dex) to the observed scatter in equation (5) is due to the uncertainty on the estimate of $L_{\rm TIR}/L_{\rm FUV}$ and β. This result confirms once more that the $L_{\rm TIR}/L_{\rm FUV}$-β relation for normal galaxies deviates from the one observed for starbursts, as pointed out by previous studies of nearby galaxies (i.e., Bell 2002; Kong et al. 2004; Boissier et al. 2005; Buat et al. 2005; Seibert et al. 2005; Burgarella et al. 2005; S. Boissier et al. 2006, in preparation) and individual H II regions in nearby galaxies (Calzetti et al. 2005).

3.1. *The Dependence on the Birthrate Parameter*

What physical mechanisms drive the difference observed in the $L_{\rm TIR}/L_{\rm FUV}$-β between normal star-forming galaxies and starbursts? Recently Kong et al. (2004) interpreted the offset as an effect of the different star formation history experienced by galaxies and proposed that the distance from the starburst IRX-UV can be predicted using the birthrate parameter b (e.g., the ratio of the current to the mean past star formation activity; Kennicutt et al. 1994). In order to test whether the perpendicular distance d_S from the $L_{\rm TIR}/L_{\rm FUV}$-β relation for starbursts correlates with the

[9] We tested this hypothesis fitting our data with functional forms similar to the ones proposed by Meurer et al. (1999) and Kong et al. (2004): no significative improvement in the scatter of this relation is obtained.

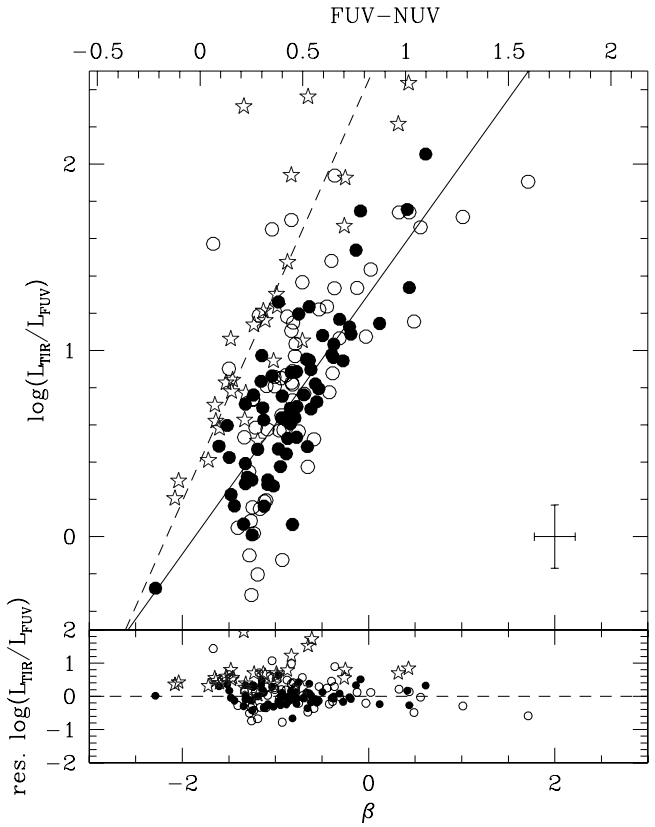

FIG. 1.—Ratio of the total infrared to FUV luminosity as a function of the ultraviolet spectral slope (the lower x-axis) and the FUV-NUV color (the upper x-axis). Open circles indicate our secondary sample, while filled circles represent the primary sample. The dashed line represents the best linear fit to starburst IRX-UV relation. The solid line indicates the best bisector linear fit for our primary sample. The stars indicate the sample of *IUE* starbursts. Mean error bars for the plotted data are shown in the lower right corner in this and in subsequent figures. The residuals from the best linear fit for normal galaxies are shown in the bottom panel. [*See the electronic edition of the Journal for a color version of this figure.*]

star formation history of normal galaxies, we compute the birthrate parameter following Boselli et al. (2001):

$$b = \frac{{\rm SFR}\, t_0 (1 - R)}{L_H (M_{\rm tot}/L_H)(1 - DM_{\rm cont})}, \quad (6)$$

where R is the fraction of gas that stellar winds reinjected into the interstellar medium during their lifetime ($\sim$0.3; Kennicutt et al. 1994), t_0 is the age of the galaxy (which we assume to be $\sim$12 Gyr), $\rm DM_{cont}$ is the dark matter contribution to the $M_{\rm tot}/L_H$ ratio at the optical radius (assumed to be 0.5; Boselli et al. 2001). We compute the H-band luminosity following Gavazzi et al. (2002a):

$$\log L_H = 11.36 - 0.4H + 2\log D \ (L_\odot),$$

where D is the distance to the source (in Mpc) and the star formation rate (SFR) from the Hα luminosity (corrected for [N II] contamination and for dust extinction using the Balmer decrement; see Appendix A), following Boselli et al. (2001), is

$${\rm SFR} = \frac{L_{\rm H\alpha}}{1.6 \times 10^{41}} \ \left(M_\odot\ {\rm yr}^{-1}\right). \quad (7)$$

Figure 2 shows the relation between the birthrate parameter (eq. [6]) and the distance from the $L_{\rm TIR}/L_{\rm FUV}$-β relation for

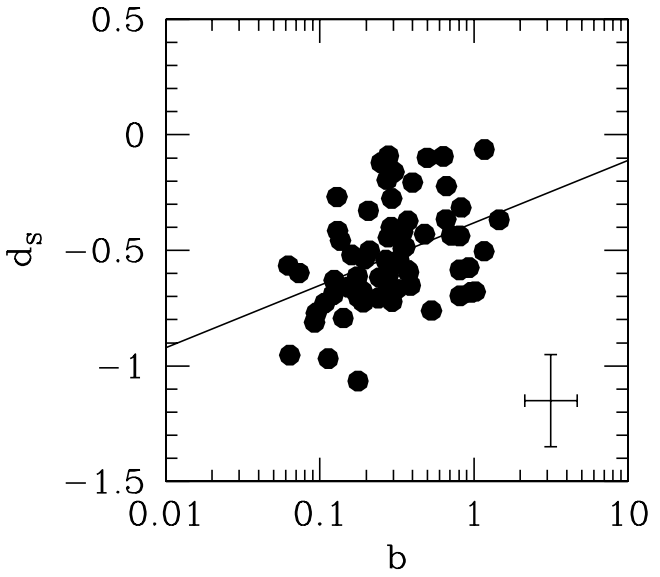

FIG. 2.—Relation between the birthrate parameter computed from the Hα emission and the distance from the L_{TIR}/L_{FUV}-β relation for starbursts. The solid line represents the best linear fit.

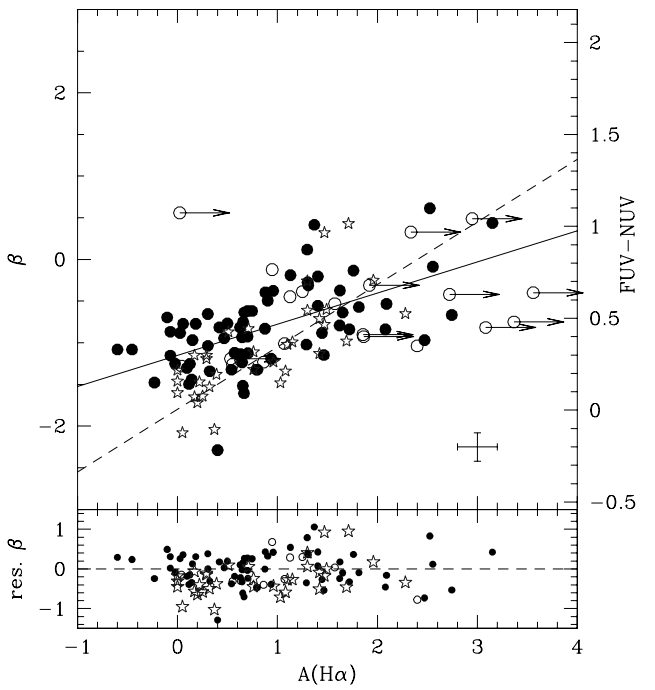

FIG. 3.—Relation between the ultraviolet spectral slope β and the Hα attenuation obtained from the Balmer decrement. Symbols are as in Fig. 1. The solid line represents the best linear fit to our primary sample (eq. [9]), while the dashed line indicates the best-fit for starburst galaxies obtained by Calzetti et al. (1994; eq. [8]). Arrows indicate galaxies for which the value of A(Hα) is a lower limit of the real value (i.e., Hβ is undetected). The residuals from the best linear fit for normal galaxies are shown in the bottom panel. [*See the electronic edition of the Journal for a color version of this figure.*]

starburst galaxies. The two quantities are correlated [$r_s \sim 0.40$, corresponding to a correlation probability $P(r_s) \sim 99.8\%$], but with a large scatter. Given the value of observational uncertainties, it is not worth trying to use the observed trend to reduce the dispersion in the L_{TIR}/L_{FUV}-β relation for normal galaxies.

This result confirms that part of the dispersion in the L_{TIR}/L_{FUV}-β relation for normal star-forming galaxies appears an effect of the different star formation history experienced by galaxies, as proposed by Kong et al. (2004).

4. THE β-A(Hα) RELATION

Calzetti et al. (1994) found a strong relationship between the ultraviolet spectral slope β and the Balmer decrement Hα/Hβ. For our starburst sample these two quantities are correlated ($r_s \sim 0.81$) as follows (see also blue stars in Fig. 3):

$$\beta = (0.75 \pm 0.10)A(\mathrm{H}\alpha) - (1.80 \pm 0.13). \quad (8)$$

This empirical relation was used by Calzetti et al. (1994) to deduce an attenuation law (the Calzetti law), often applied to high-redshift galaxies (i.e., Steidel et al. 1999; Glazebrook et al. 1999). Contrary to the L_{TIR}/L_{FUV}-β relation, the Calzetti law has not yet been tested for a sample of normal star-forming galaxies. Buat et al. (2002) showed that for normal star-forming galaxies the attenuation derived from the Calzetti law is ∼0.6 larger than the one computed from FIR/UV ratio. This result has been recently confirmed by Laird et al. (2005) on star-forming galaxies at $z \sim 1$. In order to check the Calzetti law on our sample, we use the measure of the Hα/Hβ described in the Appendix A. Figure 3 shows the relation between β and A(Hα) for our sample (*open and filled circles*). For the primary sample we obtain $r_s \sim 0.58$ [$P(r_s) > 99.9\%$] and

$$\beta = (0.37 \pm 0.07)A(\mathrm{H}\alpha) - (1.15 \pm 0.08), \quad (9)$$

flatter than for starburst galaxies (see Fig. 3). At low A(Hα) normal galaxies show on average a less steep ultraviolet spectral slope than starbursts. In addition, normal galaxies with the same value of β span a range of ∼1 mag in A(Hα). At higher attenuation the two samples appear consistent. Our results suggest that the Calzetti law cannot be applied to normal galaxies. On the contrary, the relation between β and A(Hα) for normal galaxies could be used to obtain a new attenuation law.

5. RELATIONS BETWEEN DUST ATTENUATION INDICATORS AND GLOBAL PROPERTIES

5.1. *Metallicity*

Heckman et al. (1998) have shown that the ultraviolet spectral slope and metallicity of starbursts are well correlated. To determine the metal content of our galaxies we average five different empirical determinations based on the following line ratios: $R_{23} \equiv$ ([O II] λ3727 + [O III] λ4959, 5007)/Hβ (Zaritsky et al. 1994; McGaugh 1991), [N II] λ6583/[O II] λ3727 (Kewley & Dopita 2002), [N II] λ6583/Hα (van Zee et al. 1998), and [O III] λ5007/[N II] λ6583 (Dutil & Roy 1999). The mean uncertainty in the abundances is 0.10 dex. In Figure 4 we study the relationship between the gas metallicities and the L_{TIR}/L_{FUV} ratio (*left*) and β (*right*) for normal star-forming and starburst galaxies. For normal galaxies the L_{TIR}/L_{FUV} ratio correlates [$r_s \sim 0.59, P(r_s) > 99.9\%$] with the gas abundance:

$$\log\left(\frac{L_{TIR}}{L_{FUV}}\right) = (1.37 \pm 0.24)12 + \log(\mathrm{O/H}) - (11.36 \pm 2.11), \quad (10)$$

with a dispersion of ∼0.35 ± 0.03 in log (L_{TIR}/L_{FUV}). As for the L_{TIR}/L_{FUV}-β relation normal galaxies differ from starbursts. At comparable metallicity normal galaxies show a lower L_{TIR}/L_{FUV} (lower attenuation) than starbursts, in agreement with the recent

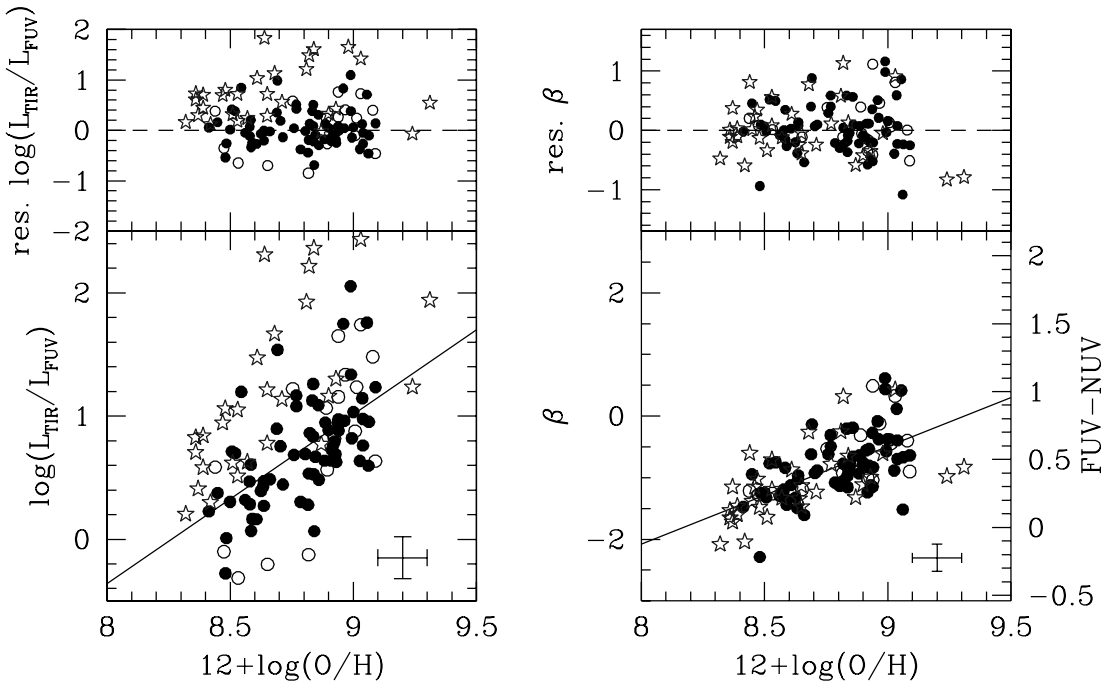

FIG. 4.—Relation between gas metallicity and the L_{TIR}/L_{FUV} ratio (*left*) or β (*right*). Symbols are as in Fig. 1. The solid lines show the best linear fit for our primary sample. The residuals from the best linear fits for normal galaxies are shown in the top panels. [*See the electronic edition of the Journal for a color version of this figure*.]

result by Boissier et al. (2004), who studied radial extinction profiles of nearby late-type galaxies using FOCA and *IRAS* observations. Unexpectedly, we find, however, that normal star-forming galaxies follow exactly the same [significant, $r_s \sim 0.58$, $P(r_s) > 99.9\%$] relationship between metallicity and ultraviolet spectral slope β determined for starbursts by Heckman et al. (1998; see Fig. 4, *right*). This might indicate that even though a normal and a starburst galaxy with similar gas metallicity have similar UV spectral slopes, they suffer from a significantly different dust attenuation, perhaps suggesting a different dust geometry (Witt & Gordon 2000). However, we stress that this effect might occur due to aperture effects in the *IUE* data: while β is not significantly contaminated by aperture effects, the L_{TIR}/L_{FUV} ratio could be overestimated, producing the observed trend (the total infrared luminosity is obtained by integrating the *IRAS* counts over the full galaxy extension, while the ultraviolet one is taken from *IUE*'s significantly smaller aperture, 20×10 arcsec^2).

This idea could be supported by the correlation [$r_s \sim 0.49$, $P(r_s) > 99.9\%$; see Fig. 5] observed between the starbursts' optical diameters and the L_{TIR}/L_{FUV} ratio, completely absent in our sample of normal galaxies [$r_s \sim 0.006$, $P(r_s) \sim 25\%$]. *GALEX* observations of starburst galaxies will rapidly solve this riddle. We also checked the dependence of the dust attenuation on the gas-to-dust ratio. Unfortunately, given the large errors on the estimate of the dust mass, we only obtain a weak relationship between the two quantities (see Appendix B).

5.2. *Luminosity*

Since it is well known that the metallicity of normal galaxies strongly correlates with galaxy luminosity (e.g., Skillman et al.

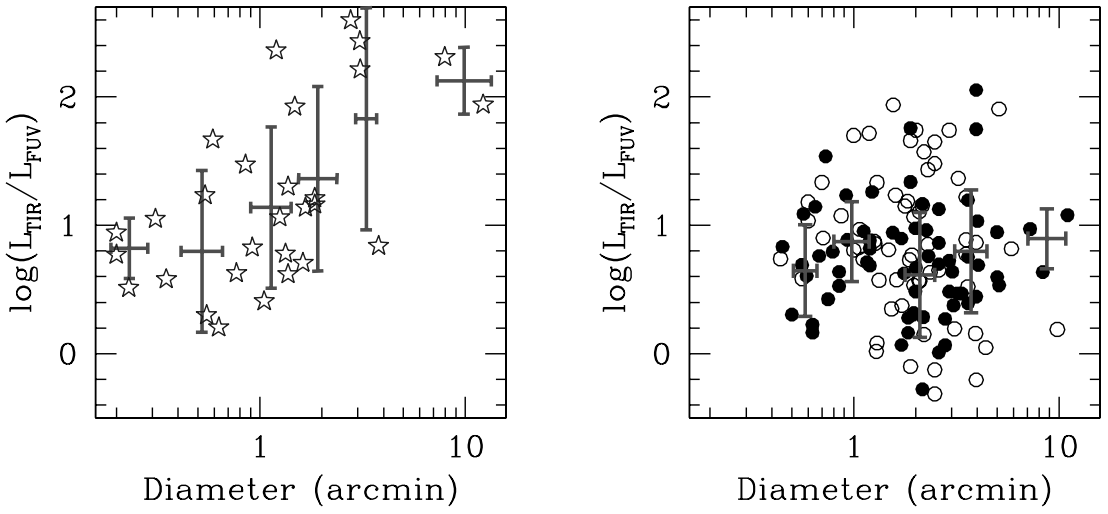

FIG. 5.—Relation between the galaxy size and the L_{TIR}/L_{FUV} ratio for starburst (*left*) and normal galaxies (*right*). Symbols are as in Fig. 1. Mean values and uncertainties in bins of 0.30 log (diameter) are given. [*See the electronic edition of the Journal for a color version of this figure*.]

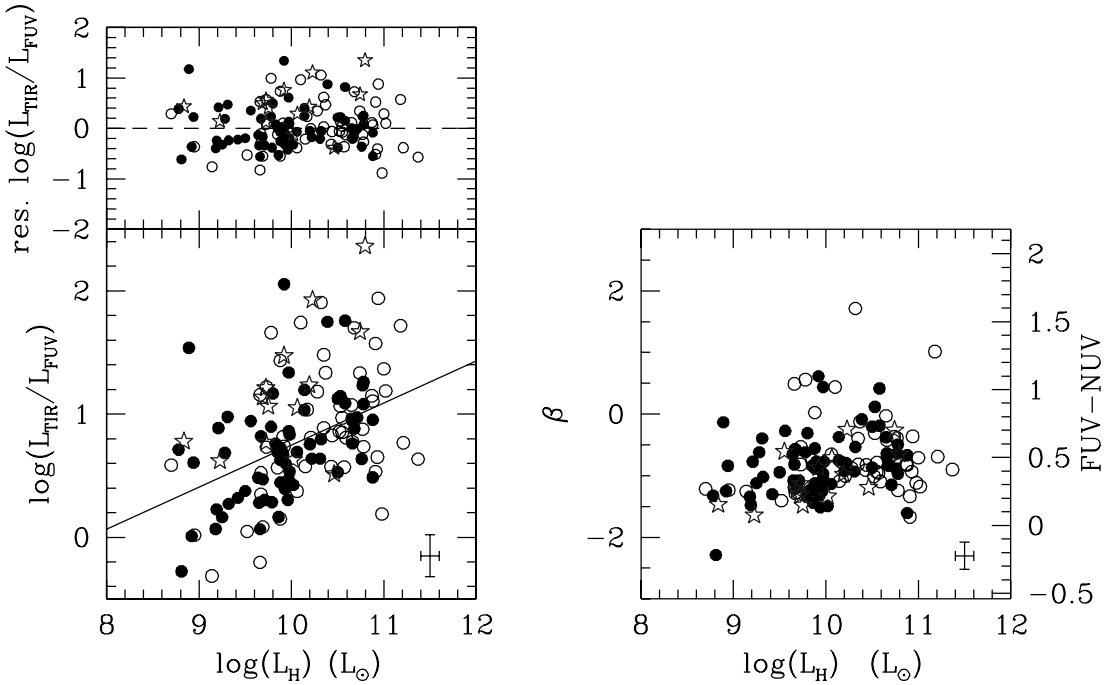

FIG. 6.—Relation between the H-band luminosity and the $L_{\rm TIR}/L_{\rm FUV}$ ratio (*left*) or β (*right*). Symbols are as in Fig. 1. The solid line shows the best linear fit for our primary sample. The residuals from the best linear fit for normal galaxies are shown in the top panel. [*See the electronic edition of the Journal for a color version of this figure*.]

1989; Zaritsky et al. 1994) and mass (e.g., Tremonti et al. 2004), it is worth considering the correlation between attenuation and galaxy luminosity. Figure 6 shows the relationships between the dust attenuation indicators $L_{\rm TIR}/L_{\rm FUV}$ and β and the H-band luminosity. The infrared to FUV ratio correlates [$r_s \sim 0.49$, $P(r_s) > 99.9\%$] with the total H-band luminosity:

$$\log\left(\frac{L_{\rm TIR}}{L_{\rm FUV}}\right) = (0.34 \pm 0.10)\log\left(\frac{L_H}{L_\odot}\right) - (2.66 \pm 0.88). \quad (11)$$

The dispersion of this relation is $\sim 0.39 \pm 0.03$ in $\log(L_{\rm TIR}/L_{\rm FUV})$. Since the H-band luminosity is proportional to the dynamical mass (Gavazzi et al. 1996), this implies a relationship between dust attenuation and dynamical mass. Also in starbursts the total H-band luminosity is correlated [$r_s \sim 0.37$, $P(r_s) \sim 99.5\%$] with the $L_{\rm TIR}/L_{\rm FUV}$ ratio and the great part of starbursts appear offset (to 99% confidence level) from the relation of normal galaxies. On the contrary, no difference is observed between the two samples in the β-L_H plot, in agreement with what observed for metallicity. Finally, Figure 7 shows the relation between the bolometric luminosity ($L_{\rm TIR} + L_{\rm FUV}$) and the dust attenuation, computed assuming that the UV emission is absorbed by dust and emitted in the FIR. The correlation coefficient [$r_s \sim 0.31$, $P(r_s) \sim 98\%$] indicates that the two quantities correlate, as for starburst galaxies (Heckman et al. 1998). This is not the case if we examine the relation between the ultraviolet spectral slope β and the bolometric luminosity (Fig. 7, *right*)—while there is no correlation [$r_s \sim 0.002$, $P(r_s) \sim 20\%$] for our sample of normal galaxies, a clear relation [$r_s \sim 0.68$, $P(r_s) > 99.9\%$] holds for starbursts. Starbursts with higher bolometric luminosity (high TIR emission) show lower ultraviolet slope, consistent with the idea that high TIR emission corresponds to high attenuation (low β).

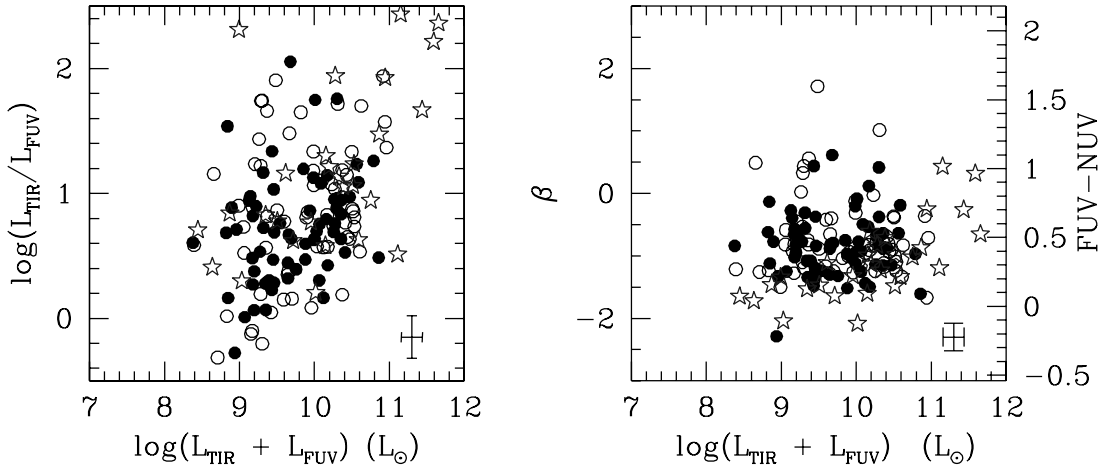

FIG. 7.—Relation between the TIR+FUV luminosity and the $L_{\rm TIR}/L_{\rm FUV}$ ratio (*left*) or β (*right*). Symbols are as in Fig. 1. [*See the electronic edition of the Journal for a color version of this figure*.]

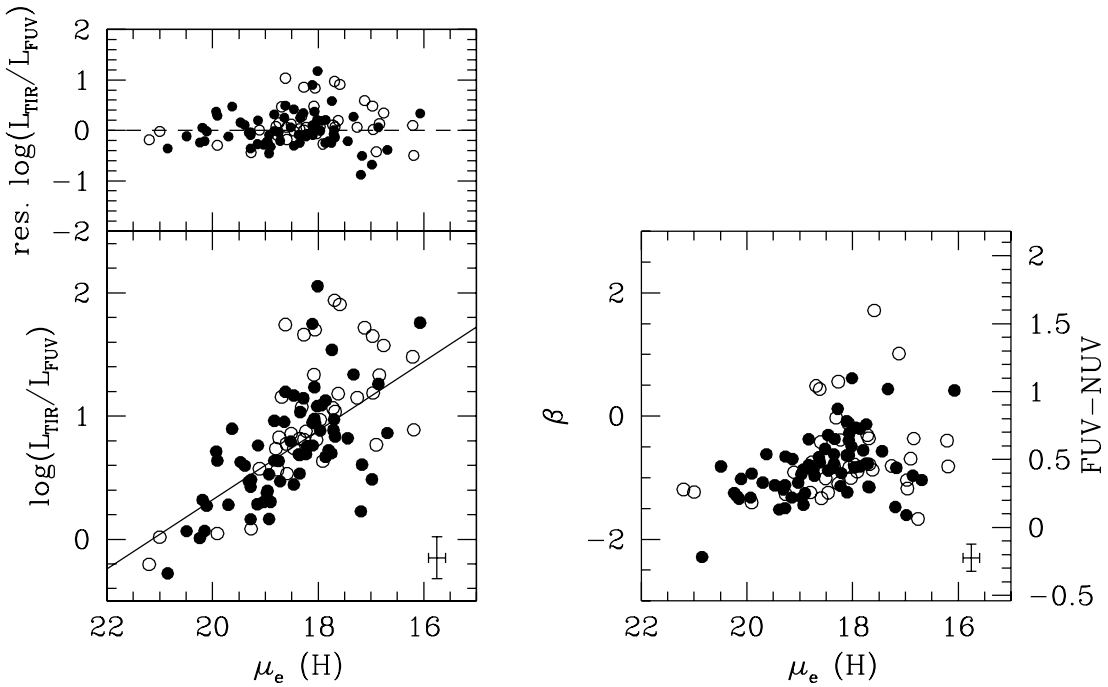

FIG. 8.—Relation between the mean H-band surface brightness (μ_e) and the $L_{\rm TIR}/L_{\rm FUV}$ ratio (*left*) or β (*right*). Symbols are as in Fig. 1. The solid line shows the best linear fit for our primary sample. The residuals from the best linear fit for normal galaxies are shown in the top panel.

5.3. *Surface Brightness*

Wang & Heckman (1996) interpreted the increase of dust attenuation with rotational velocity (or mass) as due to the variations in both the metallicity and surface density of galactic disk with galactic size. Figure 8 shows the variation of the effective H-band surface brightness (defined as the mean surface brightness within the radius that contains half of the total galaxy light) and the dust attenuation. The two quantities are strongly anticorrelated [$r_s \sim -0.63$, $P(r_s) > 99.9\%$],

$$\log\left(\frac{L_{\rm TIR}}{L_{\rm FUV}}\right) = (-0.28 \pm 0.04)\mu_e(H) + (5.92 \pm 0.81), \quad (12)$$

with a scatter of $\sim$0.34 $\pm$ 0.03 in log ($L_{\rm TIR}/L_{\rm FUV}$): $\sim$1.2 σ lower than the value obtained for H-band luminosity and consistent with the one obtained for the gas metallicity. Unfortunately, in this case we cannot compare the behavior of normal galaxies with the one of starbursts due to the lack of an estimate of μ_e for the starbursts. Does this relation indicate that UV dust extinction depends on the thickness of the stellar disk, or does it follow from the correlation between attenuation and star formation surface density? To attack this question we determine the SFR density (defined as the ratio between the SFR determined from Hα (eq. [7]) and optical galaxy area). Figure 9 shows the relation between the SFR density and log ($L_{\rm TIR}/L_{\rm FUV}$). The two quantities are correlated [$r_s \sim 0.44$, $P(r_s) > 99.9\%$] with a dispersion of $\sim$0.39 $\pm$ 0.03 in log ($L_{\rm TIR}/L_{\rm FUV}$), $\sim$1.2 σ larger than the one observed for the mean H-band surface brightness.[10] Since the contribution of observational uncertainties to the scatter in the two relations is $\sim$the same (0.18 $\pm$ 0.02), our result might suggest that the UV attenuation is primarily correlated with the thickness of stellar disk, supporting the hypothesis of Wang & Heckman (1996) that both gas metallicity and star surface density are directly connected with the physical properties of dust (i.e., quantity and spatial distribution).

[10] The difference between the two relations does not change if instead of the half-light radius, we use the total radius to estimate $\mu_e(H)$.

5.4. $L_{\rm H\alpha}/L_{\rm FUV}$ *Ratio*

Buat et al. (2002) suggested that the $L_{\rm H\alpha}/L_{\rm FUV}$ ratio could be another potential attenuation indicator but they found a scattered correlation between $L_{\rm H\alpha}/L_{\rm FUV}$ and A(FUV), confirmed by Bell (2002). This correlation is expected since both Hα and UV emission are star formation indicators. The Hα luminosity comes from stars more massive than 10 $M_\odot$ and traces the SFR in the last $\leq 10^7$ yr, while the UV luminosity comes from stars of lower mass ($M \geq 1.5\ M_\odot$) and can be used as an indicator of the SFR in the last $\approx 10^8$ yr. This means that under the condition that the star formation is approximately constant in the last $\approx 10^8$ yr, the ratio $L_{\rm H\alpha}/L_{\rm FUV}$ (corrected for attenuation) should be fixed. Thus the ratio between the extinction corrected $L_{\rm H\alpha}$ and the observed $L_{\rm FUV}$ should be a potential attenuation indicator. In Figure 10 we analyze the relationship between the dust attenuation and the $L_{\rm H\alpha}/L_{\rm FUV}$ ratio, where $L_{\rm H\alpha}$ is the Hα luminosity corrected for dust attenuation using the Balmer decrement and for the contamination of [N II]. The two quantities turn out to be strongly correlated [$r_s \sim 0.76$, $P(r_s) > 99.9\%$]:

$$\log\left(\frac{L_{\rm TIR}}{L_{\rm FUV}}\right) = (0.84 \pm 0.07)\log\left(\frac{L_{\rm H\alpha}}{L_{\rm FUV}}\right) - (0.59 \pm 0.12). \quad (13)$$

The dispersion around this relation is $\sim$0.24 $\pm$ 0.02 in log ($L_{\rm TIR}/L_{\rm FUV}$), consistent with the one observed for the log ($L_{\rm TIR}/L_{\rm FUV}$)-β relation. The high correlation and low scatter between the two quantities is expected since the two variables are mutually related: the FUV luminosity appears in both axes and $L_{\rm TIR}$ and $L_{\rm H\alpha}$ are known to be correlated (Kewley et al. 2002), explaining why in the left panel of Figure 10 starbursts and normal galaxies show the same trend. The right panel of Figure 10 shows the relation

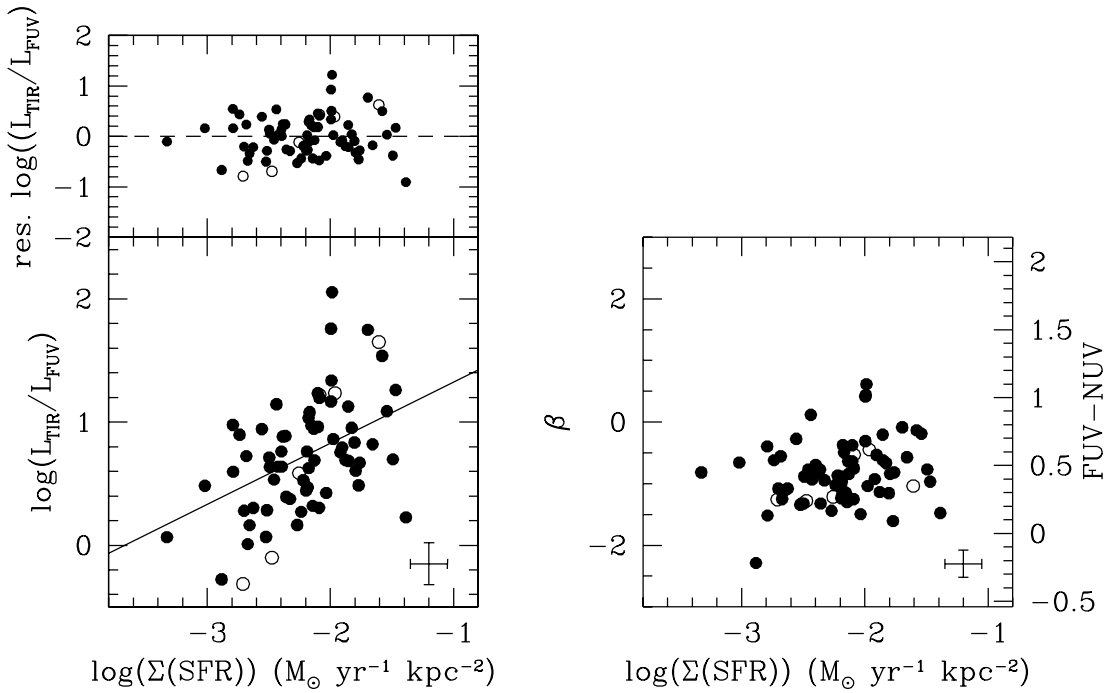

FIG. 9.—Relation between the SFR density and the L_{TIR}/L_{FUV} ratio (*left*) or β (*right*). Symbols are as in Fig. 1. The solid line shows the best linear fit for our primary sample. The residuals from the best linear fit for normal galaxies are shown in the top panel.

between the ultraviolet slope and the $L_{H\alpha}/L_{FUV}$ ratio. In this case, starbursts and normal galaxies behave differently: at any given β starbursts have an higher $L_{H\alpha}/L_{FUV}$ than normal galaxies, consistent with what expected for galaxies experiencing a burst of star formation (Iglesias-Páramo et al. 2004). A secure determination of the Balmer decrement for large samples is still a hard task, especially at high redshift, and thus we look for a relation similar to equation (13) using the observed Hα luminosity ($L_{H\alpha}^{obs}$). The $L_{H\alpha}^{obs}/L_{FUV}$ and $\log(L_{TIR}/L_{FUV})$ ratios are yet correlated (see Fig. 11), but the correlation coefficient is lower than the previous case [$r_s \sim 0.49$, $P(r_s) > 99.9\%$]. The best linear fit gives

$$\log\left(\frac{L_{TIR}}{L_{FUV}}\right) = (1.10 \pm 0.17)\log\left(\frac{L_{H\alpha}^{obs}}{L_{FUV}}\right) - (0.59 \pm 0.21), \quad (14)$$

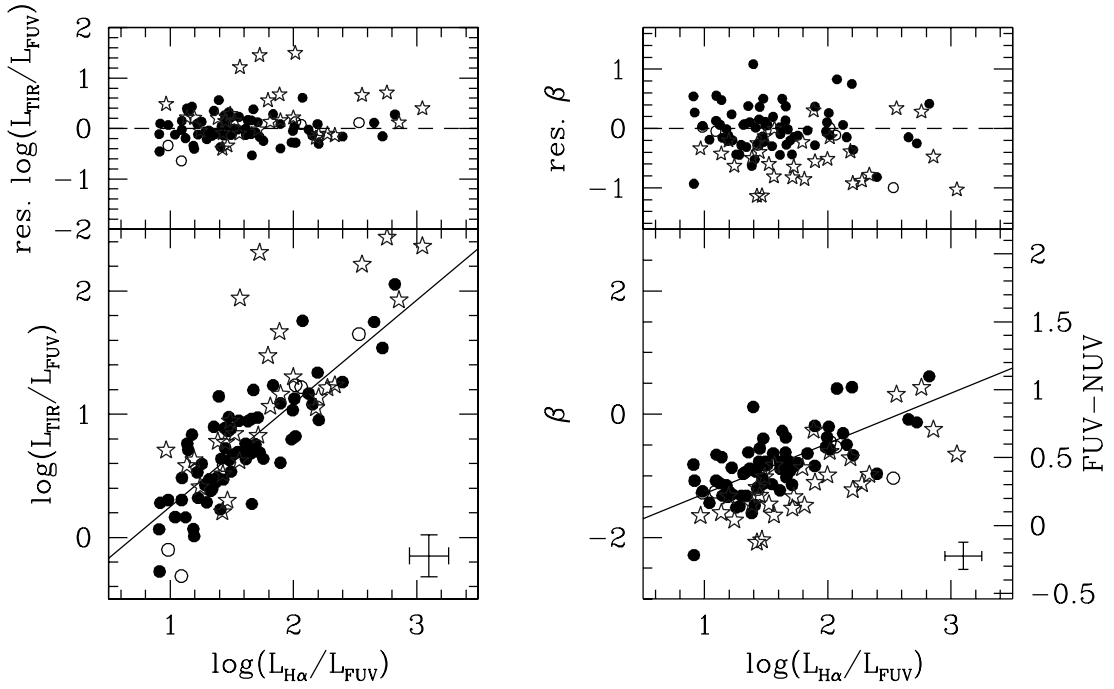

FIG. 10.—Relation between the Hα and FUV luminosity and the L_{TIR}/L_{FUV} ratio (*left*) or β (*right*). Symbols are as in Fig. 1. Hα luminosity is corrected for dust attenuation using the Balmer decrement, while the FUV flux is uncorrected. The solid lines show the best linear fit for our primary sample. The residuals from the best linear fit for normal galaxies are shown in the top panels. [*See the electronic edition of the Journal for a color version of this figure.*]

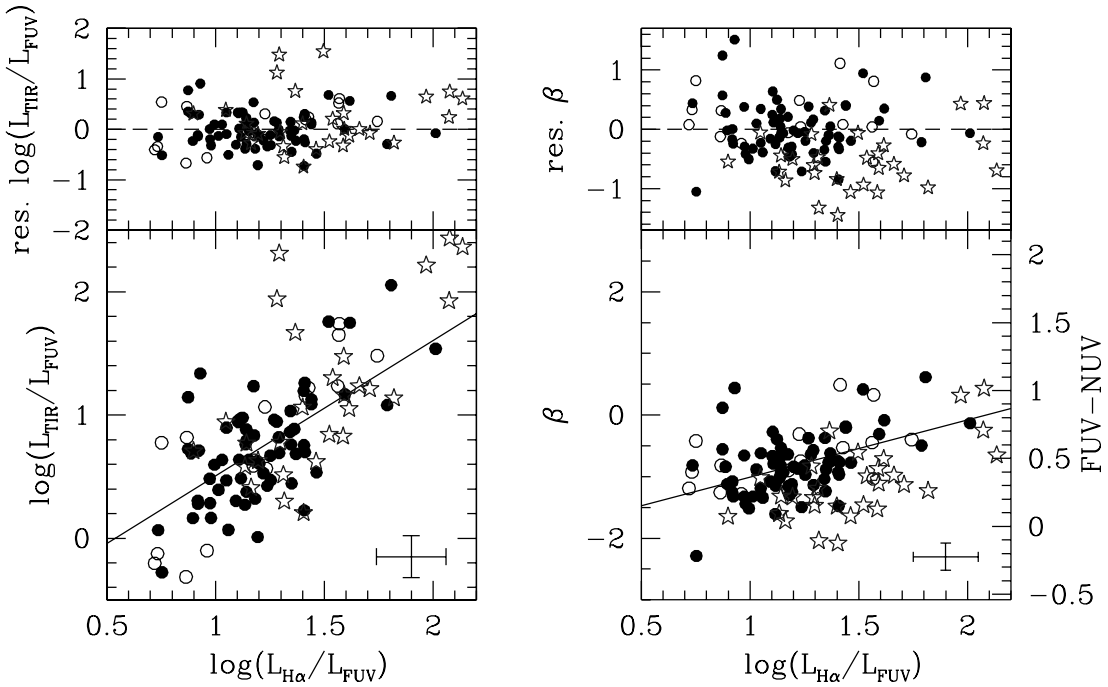

FIG. 11.—Relation between the observed Hα and FUV luminosity and the L_{TIR}/L_{FUV} ratio (*left*) or β (*right*). Symbols are as in Fig. 1. Hα luminosity is the observed value not corrected for dust attenuation. The solid lines show the best linear fit for our primary sample. The residuals from the best linear fit for normal galaxies are shown in the top panels. [*See the electronic edition of the Journal for a color version of this figure.*]

with a mean absolute deviation of $\sim$0.34 $\pm$ 0.03 ($\sim$3.3 σ higher than for eq. [14]).

6. A COOKBOOK FOR DETERMINING L_{TIR}/L_{FUV} RATIO IN OPTICALLY SELECTED GALAXIES

In this paper we investigated the relations between dust attenuation, traced by the L_{TIR}/L_{FUV} ratio, and other global properties of normal star-forming galaxies. Furthermore, we compared the dust attenuation in normal and starbursts galaxies using multiwavelength data sets. The amount of dust attenuation is found to correlate with the UV colors, gas metallicity, mass, and mean surface density, but, generally speaking, differently for normal and starburst galaxies. Determining whether this difference is real or is due to aperture effects requires the analysis of *GALEX* observations for a sample of starburst galaxies. The dispersion in the L_{TIR}/L_{FUV}-β relation correlates with the birthrate parameter b, suggesting that the observed scatter is at least partly due to differences in the star formation history. These results stress that estimating the UV dust attenuation, and consequently the SFR of normal galaxies (at high redshift in particular) is highly uncertain ($\geq$50%) when rest-frame FIR observations are not available. Moreover, the sample selection criteria could strongly affect its properties, as recently pointed out by Buat et al. (2005) and Burgarella et al. (2005). They studied the dust attenuation properties and star formation activity in UV- and FIR-selected samples, showing that the former shows correlations with global galaxy properties, such as mass and bolometric luminosity, that the FIR-selected sample does not. Their results stress that the dust attenuation properties are very heterogeneous and that L_{TIR}/L_{FUV} cannot be derived in a robust manner when FIR observations are not available. However, the present investigation has shown that among optically selected samples of normal galaxies with no nuclear activity a number of empirical relations exists, allowing us to derive the L_{TIR}/L_{FUV} ratio (and its uncertainty). Once the attenuation at UV is determined, it can be transformed to any other λ, only knowing the shape of the attenuation law and dust geometry (i.e., Calzetti et al. 1994; Gavazzi et al. 2002a; Boselli et al. 2003). In Table 1 we list all the relations, their associated rms, the mean absolute deviation (MAD) from the best fit,[11] and the Spearman correlation coefficient. Before we proceed describing our recipes, we have to investigate whether the scatter in these relations is physical or is only driven by observational uncertainties. In the latter case, in fact, our cookbook would not be very useful, since it would be valid only for observations with the same uncertainties than our data sets. For H-band luminosity, H-band surface brightness, the $L_{H\alpha}^{obs}/L_{FUV}$ ratio, and metallicity, the contribution of observational uncertainties to the observed scatter varies from $\sim$18% (rms $\sim$ 0.17 $\pm$ 0.02) for L_H to $\sim$40% (rms $\sim$ 0.21 $\pm$ 0.02) for $12 + \log(O/H)$ and $L_{H\alpha}^{obs}/L_{FUV}$: even accounting for the contribution of measurements errors, the relative difference in the scatter of these relations does not change. On the contrary, this confirms that the relation involving L_H is the one with the highest "physical" dispersion, while for the other three relations the scatter is similar. The situation is worse for the relations involving β and the $L_{H\alpha}/L_{FUV}$ ratio: the contribution of observational errors is $\sim$70%–76% ($\sim$0.21 $\pm$ 0.02). Thus it is impossible to determine which of these two relations has the lowest scatter and represents the best way to estimate dust attenuation without FIR observations. We can conclude that observational errors could account for the difference scatter observed in the relations involving β and the $L_{H\alpha}/L_{FUV}$ ratio, but not for the difference observed in all the other relations. Our results can thus be used to suggest different ways to correct for UV dust attenuation:

1a. The L_{TIR}/L_{FUV}-β relation still represents one of the best ways to quantify dust attenuation. The uncertainty in the value of $\log(L_{TIR}/L_{FUV})$ is $\sim$0.26 $\pm$ 0.03.

[11] The mean absolute deviation is less sensitive to the contribution of outliers than the standard deviation. For a Gaussian distribution the MAD is $\sim(2/\pi)^{1/2} \times$ (rms), while it is lower (higher) for a heavier (lighter) tailed distribution. As shown in Table 1 the values obtained for rms and MAD are consistent with the ones expected for a Gaussian distribution.

TABLE 1
Linear Relations Useful to Estimate the L_{TIR}/L_{FUV} Ratio [$\log(L_{TIR}/L_{FUV}) = ax + b$]

x	a	b	MAD[a]	rms[b]	r_s
β	0.70 ± 0.06	1.30 ± 0.06	0.20 ± 0.02	0.26 ± 0.02	0.76
$12 + \log(O/H)$	1.37 ± 0.24	-11.36 ± 2.11	0.26 ± 0.02	0.35 ± 0.03	0.59
$L_H/L_\odot$	0.34 ± 0.10	-2.66 ± 0.88	0.29 ± 0.03	0.39 ± 0.03	0.49
$\mu_e(H)$	-0.28 ± 0.04	5.92 ± 0.81	0.25 ± 0.02	0.34 ± 0.03	-0.63
$L_{H\alpha}/L_{FUV}$	0.84 ± 0.07	-0.59 ± 0.12	0.19 ± 0.02	0.24 ± 0.02	0.76
$L^{obs}_{H\alpha}/L_{FUV}$	1.10 ± 0.17	-0.59 ± 0.21	0.27 ± 0.02	0.34 ± 0.03	0.49

[a] Mean absolute deviation from the best fit.
[b] Standard deviation from the best fit.

1b. If the UV spectral slope β is unknown but we know $L_{H\alpha}$ (corrected for attenuation), we can obtain the ultraviolet attenuation using equation (13), with an rms of 0.24 ± 0.02. This relation is valid under the assumption that the SFR is approximately constant in the last $\approx 10^8$ yr.

2a. If we know $L^{obs}_{H\alpha}$, but no estimate of $A(H\alpha)$ is available, we can use equation (14) (rms $\sim 0.34 \pm 0.03$).

2b. If neither β nor $H\alpha$ luminosity are available, we are left with the relations with H-band surface brightness[12] (rms $\sim 0.34 \pm 0.03$) and, in the worse case,

3. H-band luminosity (rms $\sim 0.39 \pm 0.03$).

Summarizing, these relations allow us to estimate the value of the L_{TIR}/L_{FUV} ratio with an average uncertainty of $\sim$0.32 dex. This value corresponds approximately to $\sigma[A(FUV)] \sim 0.5$ mag, assuming $\log(L_{TIR}/L_{FUV}) = 1$ (the mean value for our sample) and using the model of Buat et al. (2005). This is the lowest uncertainty on the estimate of the L_{TIR}/L_{FUV} ratio in absence of FIR observations.

[12] Since we need $H\alpha$ flux to estimate metallicity, eq. (10) cannot be used in this case.

However, we caution the reader that this value holds only for an optically selected sample and that samples selected according to different criteria, especially FIR-selected, could contain higher dispersions.

We thank an unknown referee for her/his useful comments, which helped us to improve and strengthen the paper. We wish to thank Christian Bonfanti, Jorge Iglesias-Paramo, Paolo Franzetti, Akio K. Inoue, and Gerry Sanvito for useful discussions. *GALEX* is a NASA Small Explorer, launched in 2003 April. We gratefully acknowledge NASA's support for construction, operation, and science analysis for the *GALEX* mission, developed in cooperation with the Centre National d'Etudes Spatiales of France and the Korean Ministry of Science and Technology. This research has made extensive use of the GOLDMine Database and of the NASA/IPAC Extragalactic Database (NED), which is operated by the Jet Propulsion Laboratory, California Institute of Technology, under contract with the National Aeronautics and Space Administration. The authors would like to take this opportunity to thank the members of the *GALEX* SODA Team for their valiant efforts in the timely reduction of the complex observational data set covering the full expanse of the Virgo cluster.

APPENDIX A

ESTIMATE OF $A(H\alpha)$

The attenuation in the Balmer lines can be deduced from the comparison of the observed ratio $L_{H\alpha}/L_{H\beta}$ with the theoretical value of 2.86 obtained for the recombination case B, an electronic density $n_e \leq 10^4$ cm^{-3}, and temperature $\sim 10^4$ K. The variation of this value with density is negligible and with temperature is $\leq$5% (in the range between 5000 and 20,000 K; Caplan & Deharveng 1986). The underlying absorption was deblended from the $H\beta$ emission line using a multiple-component fitting procedure. To do this, the emission line is measured and subtracted from the spectra. The resulting absorption line is also measured with respect to a reference continuum. These two measurements are used as first guess in a fitting algorithm that fits jointly the emission and absorption lines to the reference continuum. For objects whose $H\beta$ is detected in emission but the deblending procedure is not applied (no absorption feature is evident), a mean additive correction for underlying absorption equal to -1.8 in flux and -1.4 Å in EW is used. These values correspond to the fraction of the (broader) absorption feature that lies under the emission line. We adopt a dust screen geometry and the Milky Way extinction curve (e.g., Kennicutt 1983; Calzetti et al. 1994). Whereas varying the extinction curves has negligible effects in the visible, the dust screen assumption seems to underestimate the extinction by $\sim$0.2 mag compared with the amount deduced from the measurements of the thermal radio continuum (Caplan & Deharveng 1986; Bell & Kennicutt 2001). We do not apply any correction for $H\alpha$ underlying absorption (Charlot & Longhetti 2001). However, since all the objects have EW($H\alpha$ + [N II]) > 3 Å, the underestimate in the value of $A(H\alpha)$ is negligible. In fact no change (at a 99% significance level) is observed comparing the best fits obtained in this work and the ones obtained adding to the $H\alpha$ the same fixed underlying absorption used for $H\beta$ when the underlying is not detected. We assume that the errors on $A(H\alpha)$ are mainly due to the uncertainty on the $H\beta$ flux. These errors represent in fact the lower limits because we do not account for the uncertainty introduced by the fitting of the lines. They range from 0.01 to 0.43 mag and are found strongly anticorrelated with EW($H\beta$) (see Gavazzi et al. 2004). Adopting the definition of the Balmer decrement as in Gavazzi et al. (2004),

$$C1(H\beta) = \frac{\log\left[(1/2.86)\left(L_{H\alpha}/L_{H\beta}\right)\right]}{0.33}. \quad \text{(A1)}$$

The $A(\mathrm{H}\alpha)$ attenuation is

$$A(\mathrm{H}\alpha) = 1.086 \frac{1}{e_{\beta\alpha} - 1} \ln\left(\frac{1}{2.86} \frac{L_{\mathrm{H}\alpha}}{L_{\mathrm{H}\beta}}\right). \quad \text{(A2)}$$

From (A1) and (A2) we obtain

$$A(\mathrm{H}\alpha) = 1.086 \frac{1}{e_{\beta\alpha} - 1} 0.33 C1(\mathrm{H}\beta) \ln(10), \quad \text{(A3)}$$

and assuming a galactic extinction law ($e_{\beta\alpha} = 1.47$) we derive

$$A(\mathrm{H}\alpha) = 1.756 C1(\mathrm{H}\beta) \quad \text{(A4)}$$

$A(\mathrm{H}\alpha) = 0.85$ mag is obtained on average, consistent with previous studies (e.g., Kennicutt 1983, 1992; Thuan & Sauvage 1992; Kewley et al. 2002). Eleven galaxies have Hβ undetected in emission, but the underlying stellar absorption is clearly detected. For them we derive a 3 σ lower limit to the Hβ flux ($f_{\mathrm{H}\beta}$) using (Gavazzi et al. 2004):

$$f_{\mathrm{H}\beta} < 3\, \mathrm{rms}_{(4500-4800)} \mathrm{H}\alpha(\mathrm{HWHM}), \quad \text{(A5)}$$

assuming that Hα and Hβ emission lines have similar HWHM (half-width at half-maximum). As shown in equation (A1), a change in the theoretical value of the $L_{\mathrm{H}\alpha}/L_{\mathrm{H}\beta}$ ratio would only produce a small ($\leq$5%) constant over- or underestimate of the ionized gas attenuation, thus leaving unchanged the shape and dispersions of the observed relations, only affecting the values of the best-fitting parameters.

APPENDIX B

DUST-TO-GAS RATIO

The correlation between attenuation and metallicity can be interpreted assuming that the ultraviolet radiation produced by star-forming regions suffers a dust attenuation increasing with the dust-to-gas ratio, which correlates with metallicity (e.g., Issa et al. 1990; Inoue 2003). In order to check this hypothesis we compute the dust-to-gas ratio following Boselli et al. (2002b). In normal galaxies the dust mass is dominated by the cold dust emitting above $\sim$200 μm. The total dust mass can be estimated provided that the 100–1000 μm FIR flux and the cold dust temperature are known. Fitting the SEDs of normal galaxies with a modified Planck law $\nu^{\beta} B_{\nu}(T_{\mathrm{dust}})$, with $\beta = 2$ (Alton et al. 2000), the total dust mass can be determined from the relation (Devereux & Young 1990):

$$M_{\mathrm{dust}} = C S_{\lambda} D^2 (e^{a/T_{\mathrm{dust}}} - 1)\, M_{\odot}, \quad \text{(B1)}$$

where C depends on the grain opacity, S_{λ} is the FIR flux at a given wavelength (in Jy), D is the distance of the galaxy (in Mpc), T_{dust} is the dust temperature, and a depends on λ. Only *IRAS* data at 60 and 100 μm are available for our sample and, given the strong contamination of the emission at 60 μm by very small grains, the 60 to 100 μm ratio does not provide a reliable measure of T_{dust} (Contursi et al. 2001). T_{dust}, determined by Alton et al. (1998) consistently with Contursi et al. (2001), seems to be independent of the UV radiation field, the metallicity, and the total luminosity (Boselli et al. 2002b). Therefore, we adopt the average value $T_{\mathrm{dust}} = 20.8 \pm 3.2$ K for all our galaxies introducing an uncertainty of $\sim$50% on the estimate of M_{dust} (eq. [B1]). We then estimate the dust mass of the sample galaxies using equation (B1) with $C = 1.27\ M_{\odot}\ \mathrm{Jy}^{-1}\ \mathrm{Mpc}^{-2}$, consistent with Contursi et al. (2001), and $a = 144$ K for $S_{\lambda} = S_{100\,\mu\mathrm{m}}$ (Devereux & Young 1990). The determination of the dust-to-gas ratio, in a way consistent with that obtained in the solar neighborhood, requires the estimate of the gas and dust surface densities, and thus of the spatial distribution of dust and gas over the disks. Unfortunately, only integrated H I and H_2 masses are available for our spatially unresolved galaxies. It is, however, reasonable to assume that the cold dust and the molecular hydrogen are as extended as the optical disk (Alton et al. 1998; Boselli et al. 2002b). To determine the mean H I surface density we adopt (Boselli et al. 2002b)

$$\log \Sigma_{\mathrm{H\,I}} = 20.92(\pm 0.17) - 0.65(\pm 0.11)[\mathrm{def(H\ I)}]\ \mathrm{cm}^{-2}$$

where def(H I) is the galaxy H I deficiency. Thus the dust-to-gas ratio is obtained from the ratio of the dust surface density to the sum of molecular and neutral hydrogen surface densities. In Figure 12 we compare the relation between the $L_{\mathrm{TIR}}/L_{\mathrm{FUV}}$ ratio (*left*) and β (*right*) with the dust-to-gas ratio. The gas-to-dust ratio barely correlates with the $L_{\mathrm{TIR}}/L_{\mathrm{FUV}}$ ratio ($R \sim 0.38$). Contrary to metallicity, we do not find a significant correlation ($R \sim 0.11$) with the ultraviolet spectral slope. This is probably due to the high uncertainty in our estimate of M_{dust} consequent to assuming the same temperature for all our galaxies ($M_{\mathrm{dust}} \propto e^{a/T_{\mathrm{dust}}}$, and thus small errors [$\sim$15%] on T_{dust} propagate onto $\sim$50% errors on M_{dust}).

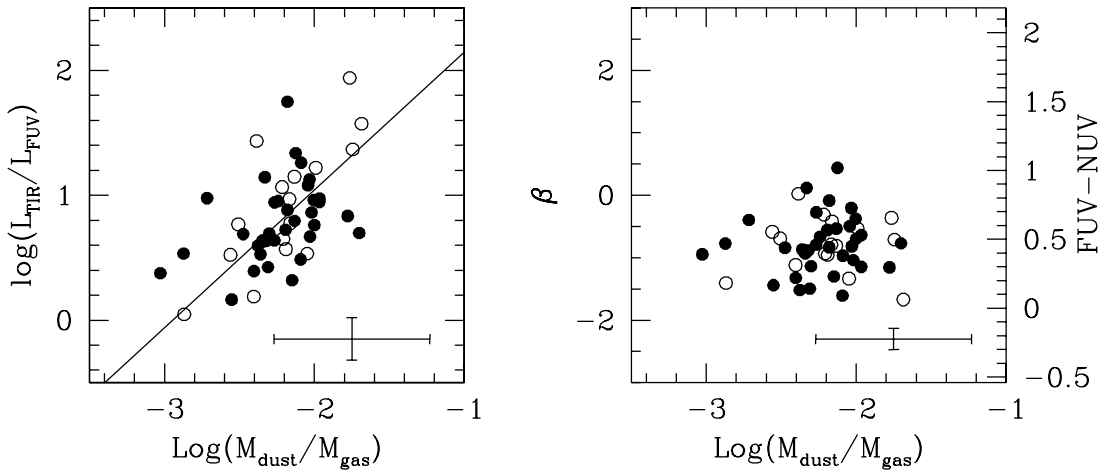

FIG. 12.—Relation between the gas-to-dust ratio and the L_{TIR}/L_{FUV} ratio (*left*) or β (*right*). Symbols are as in Fig. 1. The solid line shows the best linear fit for our primary sample.

REFERENCES

Abazajian, K., et al. 2005, AJ, 129, 1755
Alton, P. B., Xilouris, E. M., Bianchi, S., Davies, J., & Kylafis, N. 2000, A&A, 356, 795
Alton, P. B., et al. 1998, A&A, 335, 807
Bell, E. F. 2002, ApJ, 577, 150
Bell, E. F., & Kennicutt, R. C. 2001, ApJ, 548, 681
Binggeli, B., Sandage, A., & Tammann, G. A. 1985, AJ, 90, 1681
Boissier, S., Boselli, A., Buat, V., Donas, J., & Milliard, B. 2004, A&A, 424, 465
Boissier, S., et al. 2005, ApJ, 619, L83
Boselli, A., & Gavazzi, G. 2002, A&A, 386, 124
Boselli, A., Gavazzi, G., Donas, J., & Scodeggio, M. 2001, AJ, 121, 753
Boselli, A., Gavazzi, G., & Sanvito, G. 2003, A&A, 402, 37
Boselli, A., Iglesias-Páramo, J., Vílchez, J. M., & Gavazzi, G. 2002a, A&A, 386, 134
Boselli, A., Lequeux, J., & Gavazzi, G. 2002b, A&A, 384, 33
Buat, V. 1992, A&A, 264, 444
Buat, V., Boselli, A., Gavazzi, G., & Bonfanti, C. 2002, A&A, 383, 801
Buat, V., Donas, J., Milliard, B., & Xu, C. 1999, A&A, 352, 371
Buat, V., & Xu, C. 1996, A&A, 306, 61
Buat, V., et al. 2005, ApJ, 619, L51
Burgarella, D., Buat, V., & Iglesias-Páramo, J. 2005, MNRAS, 360, 1413
Burstein, D., & Heiles, C. 1982, AJ, 87, 1165
Calzetti, D. 1997, AJ, 113, 162
———. 2001, PASP, 113, 1449
Calzetti, D., Bohlin, R. C., Kinney, A. L., Storchi-Bergmann, T., & Heckman, T. M. 1995, ApJ, 443, 136
Calzetti, D., Kinney, A. L., & Storchi-Bergmann, T. 1994, ApJ, 429, 582
Calzetti, D., et al. 2005, ApJ, 633, 871
Caplan, J., & Deharveng, L. 1986, A&A, 155, 297
Charlot, S., & Fall, S. M. 2000, ApJ, 539, 718
Charlot, S., & Longhetti, M. 2001, MNRAS, 323, 887
Colless, M., et al. 2001, MNRAS, 328, 1039
Contursi, A., et al. 2001, A&A, 365, 11
Dale, D. A., Helou, G., Contursi, A., Silbermann, N. A., & Kolhatkar, S. 2001, ApJ, 549, 215
Devereux, N. A., & Young, J. S. 1990, ApJ, 359, 42
Dutil, Y., & Roy, J. 1999, ApJ, 516, 62
Gavazzi, G., Bonfanti, C., Sanvito, G., Boselli, A., & Scodeggio, M. 2002a, ApJ, 576, 135
Gavazzi, G., Boselli, A., Donati, A., Franzetti, P., & Scodeggio, M. 2003, A&A, 400, 451
Gavazzi, G., Boselli, A., Pedotti, P., Gallazzi, A., & Carrasco, L. 2002b, A&A, 386, 114
Gavazzi, G., Boselli, A., Scodeggio, M., Pierini, D., & Belsole, E. 1999, MNRAS, 304, 595
Gavazzi, G., Catinella, B., Carrasco, L., Boselli, A., & Contursi, A. 1998, AJ, 115, 1745
Gavazzi, G., Franzetti, P., Scodeggio, M., Boselli, A., & Pierini, D. 2000, A&A, 361, 863
Gavazzi, G., Pierini, D., & Boselli, A. 1996, A&A, 312, 397
Gavazzi, G., Zaccardo, A., Sanvito, G., Boselli, A., & Bonfanti, C. 2004, A&A, 417, 499
Gavazzi, G., et al. 2005, A&A, 430, 411
———. 2006, A&A, in press
Glazebrook, K., Blake, C., Economou, F., Lilly, S., & Colless, M. 1999, MNRAS, 306, 843
Gordon, K. D., Clayton, G. C., Witt, A. N., & Misselt, K. A. 2000, ApJ, 533, 236
Heckman, T. M., Robert, C., Leitherer, C., Garnett, D. R., & van der Rydt, F. 1998, ApJ, 503, 646
Helou, G., Khan, I. R., Malek, L., & Boehmer, L. 1988, ApJS, 68, 151
Iglesias-Páramo, J., Boselli, A., Cortese, L., Vílchez, J. M., & Gavazzi, G. 2002, A&A, 384, 383
Iglesias-Páramo, J., Boselli, A., Gavazzi, G., & Zaccardo, A. 2004, A&A, 421, 887
Inoue, A. K. 2003, PASJ, 55, 901
Isobe, T., Feigelson, E. D., Akritas, M. G., & Babu, G. J. 1990, ApJ, 364, 104
Issa, M. R., MacLaren, I., & Wolfendale, A. W. 1990, A&A, 236, 237
Kauffmann, G., et al. 2003, MNRAS, 346, 1055
Kennicutt, R. C. 1983, ApJ, 272, 54
———. 1992, ApJ, 388, 310
Kennicutt, R. C., Tamblyn, P., & Congdon, C. E. 1994, ApJ, 435, 22
Kewley, L. J., & Dopita, M. A. 2002, ApJS, 142, 35
Kewley, L. J., Geller, M. J., Jansen, R. A., & Dopita, M. A. 2002, AJ, 124, 3135
Kewley, L. J., Jansen, R. A., & Geller, M. J. 2005, PASP, 117, 227
Kong, X., Charlot, S., Brinchmann, J., & Fall, S. M. 2004, MNRAS, 349, 769
Laird, E. S., Nandra, K., Adelberger, K. L., Steidel, C. C., & Reddy, N. A. 2005, MNRAS, 359, 47
Leitherer, C., & Heckman, T. M. 1995, ApJS, 96, 9
Martin, D. C., et al. 2005, ApJ, 619, L1
McGaugh, S. S. 1991, ApJ, 380, 140
Meurer, G. R., Heckman, T. M., & Calzetti, D. 1999, ApJ, 521, 64
Meurer, G. R., et al. 1995, AJ, 110, 2665
Morrissey, P., et al. 2005, ApJ, 619, L7
Osterbrock, D. E. 1989, Astrophysics of Gaseous Nebulae and Active Galactic Nuclei (Mill Valley: University Science Books)
Panuzzo, P., Bressan, A., Granato, G. L., Silva, L., & Danese, L. 2003, A&A, 409, 99
Seibert, M., et al. 2005, ApJ, 619, L55
Skillman, E. D., Kennicutt, R. C., & Hodge, P. W. 1989, ApJ, 347, 875
Steidel, C. C., Adelberger, K. L., Giavalisco, M., Dickinson, M., & Pettini, M. 1999, ApJ, 519, 1
Thuan, T. X., & Sauvage, M. 1992, A&AS, 92, 749
Tremonti, C. A., et al. 2004, ApJ, 613, 898
van Zee, L., Salzer, J. J., Haynes, M. P., O'Donoghue, A. A., & Balonek, T. J. 1998, AJ, 116, 2805
Wang, B., & Heckman, T. M. 1996, ApJ, 457, 645
Witt, A. N., & Gordon, K. D. 2000, ApJ, 528, 799
Xu, C., & Buat, V. 1995, A&A, 293, L65
Zaritsky, D., Kennicutt, R. C., & Huchra, J. P. 1994, ApJ, 420, 87
Zwicky, F., Herzog, E., & Wild, P. 1961, Catalogue of Galaxies and of Clusters of Galaxies (Pasadena: Caltech)